

**Search for Associated Production
of Massive States
Decaying into Two Photons
in e^+e^- Annihilations at $\sqrt{s} = 88 - 209$ GeV**

The OPAL Collaboration

Abstract

A search is performed for production of short-lived particles in $e^+e^- \rightarrow XY$, with $X \rightarrow \gamma\gamma$ and $Y \rightarrow f\bar{f}$, for scalar X and scalar or vector Y . Model-independent limits in the range of 25-60 femtobarns are presented on $\sigma(e^+e^- \rightarrow XY) \times B(X \rightarrow \gamma\gamma) \times B(Y \rightarrow f\bar{f})$ for centre-of-mass energies in the range 205–207 GeV. The data from all LEP centre-of-mass energies 88–209 GeV are also interpreted in the context of fermiophobic Higgs boson models, for which a lower mass limit of 105.5 GeV is obtained for a “benchmark” fermiophobic Higgs boson.

(Submitted to Physics Letters B)

The OPAL Collaboration

G. Abbiendi², C. Ainsley⁵, P.F. Åkesson³, G. Alexander²², J. Allison¹⁶, P. Amaral⁹,
G. Anagnostou¹, K.J. Anderson⁹, S. Arcelli², S. Asai²³, D. Axen²⁷, G. Azuelos^{18,a}, I. Bailey²⁶,
E. Barberio⁸, R.J. Barlow¹⁶, R.J. Batley⁵, P. Bechtel²⁵, T. Behnke²⁵, K.W. Bell²⁰, P.J. Bell¹,
G. Bella²², A. Bellerive⁶, G. Benelli⁴, S. Bethke³², O. Biebel³², I.J. Bloodworth¹, O. Boeriu¹⁰,
P. Bock¹¹, D. Bonacorsi², M. Boutemeur³¹, S. Braibant⁸, L. Brigliadori², R.M. Brown²⁰,
K. Buesser²⁵, H.J. Burckhart⁸, J. Cammin³, S. Campana⁴, R.K. Carnegie⁶, B. Caron²⁸,
A.A. Carter¹³, J.R. Carter⁵, C.Y. Chang¹⁷, D.G. Charlton^{1,b}, I. Cohen²², A. Csilling^{8,g},
M. Cuffiani², S. Dado²¹, G.M. Dallavalle², S. Dallison¹⁶, A. De Roeck⁸, E.A. De Wolf⁸,
K. Desch²⁵, M. Donkers⁶, J. Dubbert³¹, E. Duchovni²⁴, G. Duckeck³¹, I.P. Duerdoth¹⁶,
E. Elfgrén¹⁸, E. Etzion²², F. Fabbri², L. Feld¹⁰, P. Ferrari¹², F. Fiedler³¹, I. Fleck¹⁰, M. Ford⁵,
A. Frey⁸, A. Fürtjes⁸, P. Gagnon¹², J.W. Gary⁴, G. Gaycken²⁵, C. Geich-Gimbel³,
G. Giacomelli², P. Giacomelli², M. Giunta⁴, J. Goldberg²¹, E. Gross²⁴, J. Grunhaus²²,
M. Gruwé⁸, P.O. Günther³, A. Gupta⁹, C. Hajdu²⁹, M. Hamann²⁵, G.G. Hanson⁴, K. Harder²⁵,
A. Harel²¹, M. Harin-Dirac⁴, M. Hauschild⁸, J. Hauschildt²⁵, C.M. Hawkes¹, R. Hawkings⁸,
R.J. Hemingway⁶, C. Hensel²⁵, G. Herten¹⁰, R.D. Heuer²⁵, J.C. Hill⁵, K. Hoffman⁹, R.J. Homer¹,
D. Horváth^{29,c}, R. Howard²⁷, P. Hüntemeyer²⁵, P. Igo-Kemenes¹¹, K. Ishii²³, H. Jeremie¹⁸,
P. Jovanovic¹, T.R. Junk⁶, N. Kanaya²⁶, J. Kanzaki²³, G. Karapetian¹⁸, D. Karlen⁶,
V. Kartvelishvili¹⁶, K. Kawagoe²³, T. Kawamoto²³, R.K. Keeler²⁶, R.G. Kellogg¹⁷,
B.W. Kennedy²⁰, D.H. Kim¹⁹, K. Klein¹¹, A. Klier²⁴, S. Kluth³², T. Kobayashi²³, M. Kobel³,
T.P. Kokott³, S. Komamiya²³, L. Kormos²⁶, R.V. Kowalewski²⁶, T. Krämer²⁵, T. Kress⁴,
P. Krieger^{6,l}, J. von Krogh¹¹, D. Krop¹², M. Kupper²⁴, P. Kyberd¹³, G.D. Lafferty¹⁶,
H. Landsman²¹, D. Lanske¹⁴, J.G. Layter⁴, A. Leins³¹, D. Lellouch²⁴, J. Letts¹², L. Levinson²⁴,
J. Lillich¹⁰, S.L. Lloyd¹³, F.K. Loebinger¹⁶, J. Lu²⁷, J. Ludwig¹⁰, A. Macpherson^{28,i}, W. Mader³,
S. Marcellini², T.E. Marchant¹⁶, A.J. Martin¹³, J.P. Martin¹⁸, G. Masetti², T. Mashimo²³,
P. Mättig^m, W.J. McDonald²⁸, J. McKenna²⁷, T.J. McMahon¹, R.A. McPherson²⁶, F. Meijers⁸,
P. Mendez-Lorenzo³¹, W. Menges²⁵, F.S. Merritt⁹, H. Mes^{6,a}, A. Michelini², S. Mihara²³,
G. Mikenberg²⁴, D.J. Miller¹⁵, S. Moed²¹, W. Mohr¹⁰, T. Mori²³, A. Mutter¹⁰, K. Nagai¹³,
I. Nakamura²³, H.A. Neal³³, R. Nisius⁸, S.W. O’Neale¹, A. Oh⁸, A. Okpara¹¹, M.J. Oreglia⁹,
S. Orito²³, C. Pahl³², G. Pásztor^{8,g}, J.R. Pater¹⁶, G.N. Patrick²⁰, J.E. Pilcher⁹, J. Pinfold²⁸,
D.E. Plane⁸, B. Poli², J. Polok⁸, O. Pooth¹⁴, M. Przybycień^{8,n}, A. Quadt³, K. Rabbertz⁸,
C. Rembser⁸, P. Renkel²⁴, H. Rick⁴, J.M. Roney²⁶, S. Rosati³, Y. Rozen²¹, K. Runge¹⁰,
D.R. Rust¹², K. Sachs⁶, T. Saeki²³, O. Sahr³¹, E.K.G. Sarkisyan^{8,j}, A.D. Schaile³¹, O. Schaile³¹,
P. Scharff-Hansen⁸, J. Schieck³², T. Schoerner-Sadenius⁸, M. Schröder⁸, M. Schumacher³,
C. Schwick⁸, W.G. Scott²⁰, R. Seuster^{14,f}, T.G. Shears^{8,h}, B.C. Shen⁴,
C.H. Shepherd-Themistocleous⁵, P. Sherwood¹⁵, G. Siroli², A. Skuja¹⁷, A.M. Smith⁸, R. Sobie²⁶,
S. Söldner-Rembold^{10,d}, S. Spagnolo²⁰, F. Spano⁹, A. Stahl³, K. Stephens¹⁶, D. Strom¹⁹,
R. Ströhmer³¹, S. Tarem²¹, M. Tasevsky⁸, R.J. Taylor¹⁵, R. Teuscher⁹, M.A. Thomson⁵,
E. Torrence¹⁹, D. Tova²³, P. Tran⁴, T. Trefzger³¹, A. Tricoli², I. Trigger⁸, Z. Trócsányi^{30,e},
E. Tsur²², A.S. Turcot^{9,o}, M.F. Turner-Watson¹, I. Ueda²³, B. Ujvári^{30,e}, B. Vachon²⁶,
C.F. Vollmer³¹, P. Vannerem¹⁰, M. Verzocchi¹⁷, H. Voss⁸, J. Vossebeld⁸, D. Waller⁶, C.P. Ward⁵,
D.R. Ward⁵, P.M. Watkins¹, A.T. Watson¹, N.K. Watson¹, P.S. Wells⁸, T. Wengler⁸,
N. Vermes³, D. Wetterling¹¹, G.W. Wilson^{16,k}, J.A. Wilson¹, G. Wolf²⁴, T.R. Wyatt¹⁶,
S. Yamashita²³, V. Zacek¹⁸, D. Zer-Zion⁴, L. Zivkovic²⁴

¹School of Physics and Astronomy, University of Birmingham, Birmingham B15 2TT, UK

²Dipartimento di Fisica dell’ Università di Bologna and INFN, I-40126 Bologna, Italy

- ³Physikalisches Institut, Universität Bonn, D-53115 Bonn, Germany
- ⁴Department of Physics, University of California, Riverside CA 92521, USA
- ⁵Cavendish Laboratory, Cambridge CB3 0HE, UK
- ⁶Ottawa-Carleton Institute for Physics, Department of Physics, Carleton University, Ottawa, Ontario K1S 5B6, Canada
- ⁸CERN, European Organisation for Nuclear Research, CH-1211 Geneva 23, Switzerland
- ⁹Enrico Fermi Institute and Department of Physics, University of Chicago, Chicago IL 60637, USA
- ¹⁰Fakultät für Physik, Albert-Ludwigs-Universität Freiburg, D-79104 Freiburg, Germany
- ¹¹Physikalisches Institut, Universität Heidelberg, D-69120 Heidelberg, Germany
- ¹²Indiana University, Department of Physics, Swain Hall West 117, Bloomington IN 47405, USA
- ¹³Queen Mary and Westfield College, University of London, London E1 4NS, UK
- ¹⁴Technische Hochschule Aachen, III Physikalisches Institut, Sommerfeldstrasse 26-28, D-52056 Aachen, Germany
- ¹⁵University College London, London WC1E 6BT, UK
- ¹⁶Department of Physics, Schuster Laboratory, The University, Manchester M13 9PL, UK
- ¹⁷Department of Physics, University of Maryland, College Park, MD 20742, USA
- ¹⁸Laboratoire de Physique Nucléaire, Université de Montréal, Montréal, Quebec H3C 3J7, Canada
- ¹⁹University of Oregon, Department of Physics, Eugene OR 97403, USA
- ²⁰CLRC Rutherford Appleton Laboratory, Chilton, Didcot, Oxfordshire OX11 0QX, UK
- ²¹Department of Physics, Technion-Israel Institute of Technology, Haifa 32000, Israel
- ²²Department of Physics and Astronomy, Tel Aviv University, Tel Aviv 69978, Israel
- ²³International Centre for Elementary Particle Physics and Department of Physics, University of Tokyo, Tokyo 113-0033, and Kobe University, Kobe 657-8501, Japan
- ²⁴Particle Physics Department, Weizmann Institute of Science, Rehovot 76100, Israel
- ²⁵Universität Hamburg/DESY, Institut für Experimentalphysik, Notkestrasse 85, D-22607 Hamburg, Germany
- ²⁶University of Victoria, Department of Physics, P O Box 3055, Victoria BC V8W 3P6, Canada
- ²⁷University of British Columbia, Department of Physics, Vancouver BC V6T 1Z1, Canada
- ²⁸University of Alberta, Department of Physics, Edmonton AB T6G 2J1, Canada
- ²⁹Research Institute for Particle and Nuclear Physics, H-1525 Budapest, P O Box 49, Hungary
- ³⁰Institute of Nuclear Research, H-4001 Debrecen, P O Box 51, Hungary
- ³¹Ludwig-Maximilians-Universität München, Sektion Physik, Am Coulombwall 1, D-85748 Garching, Germany
- ³²Max-Planck-Institute für Physik, Föhringer Ring 6, D-80805 München, Germany
- ³³Yale University, Department of Physics, New Haven, CT 06520, USA

^a and at TRIUMF, Vancouver, Canada V6T 2A3

^b and Royal Society University Research Fellow

^c and Institute of Nuclear Research, Debrecen, Hungary

^d and Heisenberg Fellow

^e and Department of Experimental Physics, Lajos Kossuth University, Debrecen, Hungary

^f and MPI München

^g and Research Institute for Particle and Nuclear Physics, Budapest, Hungary

^h now at University of Liverpool, Dept of Physics, Liverpool L69 3BX, UK

ⁱ and CERN, EP Div, 1211 Geneva 23

^j and Universitaire Instelling Antwerpen, Physics Department, B-2610 Antwerpen, Belgium

^k now at University of Kansas, Dept of Physics and Astronomy, Lawrence, KS 66045, USA

^l now at University of Toronto, Dept of Physics, Toronto, Canada
^m current address Bergische Universität, Wuppertal, Germany
ⁿ and University of Mining and Metallurgy, Cracow, Poland
^o now at Brookhaven National Laboratory, Upton, NY 11973, USA

1 Introduction

This paper presents the results of two types of search for the production of a di-photon system recoiling from another massive scalar or vector object. The searches are sensitive to the processes $e^+e^- \rightarrow XY$, with $X \rightarrow \gamma\gamma$ and $Y \rightarrow f\bar{f}$, where $f\bar{f}$ is a hadronic system (jets), a pair of charged leptons, or neutrinos resulting in missing energy. In the *general* search mode X must be a scalar, Y can be any scalar or vector particle of any mass, and both particles must be short-lived so that they decay close to the interaction point. The other search mode is referred to as the h^0Z^0 search; it requires Y to be a Z^0 boson and is applied to data taken at all energies. The data used for these searches were recorded by the OPAL detector at centre-of-mass energies (E_{cm}) 88 – 209 GeV, the entire energy range achieved at LEP.

These searches are largely motivated by “fermiophobic” scenarios where one of the Higgs bosons decays primarily into a boson pair. In the fermiophobic interpretation, Y would be a Z^0 and X a Higgs boson decaying into two photons. Indeed, the Higgs boson predicted in the Standard Model decays into two photons via a quark- or W-boson loop [1], but with a rate too low for observation of the process at LEP luminosities. Processes $e^+e^- \rightarrow h^0Z^0 \rightarrow \gamma\gamma f\bar{f}$ at near-Standard Model production rate and having large di-photon branching ratios have been predicted in a number of alternative theories [2–6]; here h^0 refers to the lightest neutral boson where extended Higgs sector models are discussed. A particularly natural situation for fermiophobic Higgs bosons occurs in two Higgs doublet models (2HDM) [7] of “Type-I”, where one Higgs doublet couples only to bosons. Because there are different fermiophobic models, it is not possible to present search results for the entire parameter space of the various theories. In the present paper a benchmark fermiophobic model is defined as having Standard Model production strength and a Higgs boson di-photon branching fraction calculated by turning off the fermion couplings to the Higgs boson in the Standard Model.

The OPAL Collaboration has presented searches similar to those reported here for LEP energies up to $E_{\text{cm}} = 189$ GeV [8–11]; this paper extends those searches with the addition of data taken at $E_{\text{cm}} = 192–209$ GeV. Fermiophobic Higgs boson searches have also been presented by other LEP collaborations [12–14] and by hadron collider experiments [15, 16]. To date, no evidence of a fermiophobic Higgs boson has been seen.

2 Data, Simulated Backgrounds and Signals

The data used in this analysis were recorded using the OPAL detector [17] at LEP. The 1999 data consisted of 217.0 ± 0.7 pb⁻¹ collected at $E_{\text{cm}} = 192–202$ GeV. The 2000 LEP data consisted of 211.1 ± 0.8 pb⁻¹ collected at $E_{\text{cm}} = 200–209$ GeV, with the majority of the data taken at 205 and 207 GeV. The data sets are summarized in Table 1.

The backgrounds from Standard Model processes were modelled using Monte Carlo simulations at $\sqrt{s} = 192, 196, 202,$ and 206 GeV for the 1999 and 2000 data. Simulated events were processed using the full OPAL detector Monte Carlo [18] and analysed in the same manner as the data. The full-detector simulations were reweighted for the \sqrt{s} distribution of the data using the Monte Carlo generators.

The dominant background to this search arises from the emission of two energetic initial state radiation (ISR) photons. This process was simulated using the KK2f/CEEX [19] generator with hadronisation and fragmentation by PYTHIA 6.125 [20]. The CEEX modelling of ISR employs full second-order QED corrections to the matrix element, and applies coherent exponentiation of the QED corrections from interference between ISR and final-state radiation. Four-fermion processes were modelled using the grc4f [21] and KORALW [22] generators. Two-lepton final states

were simulated using BHWIDE [23], TEEGG [24] and KORALZ [25]. The NUNUGPV [26] program was used to generate events of the type $e^+e^- \rightarrow \nu\bar{\nu}\gamma\gamma(\gamma)$. The process $e^+e^- \rightarrow \gamma\gamma$ was simulated using the RADCOR generator [27]. Tau lepton decays were modelled using Tauola 2.4 [28].

The process $e^+e^- \rightarrow h^0Z^0$, $h^0 \rightarrow \gamma\gamma$ was simulated for each Z^0 decay channel using the HZHA3 generator [29]. For the *general* search, which is applied to the data taken in 2000 only, the role of the Z^0 was replaced by scalar or vector particles having masses from 10 – 200 GeV. Efficiencies for signals were estimated by generating Monte Carlo for both scalar and vector signals in mass steps of 5 GeV; the scalar and vector efficiencies agreed within systematic errors and therefore are not treated as separate cases.

3 Event Selection

The analysis described in the following is identical to the one used in the paper for OPAL data taken at 189 GeV [8]. Slightly different analysis cuts were used on the lower energy data sets, as described in the earlier publications [9–11].

Events were selected if there were at least two photons recoiling from some other system decaying into one of the following three topologies:

- (A) a $q\bar{q}$ pair (“Hadronic Channel”), or
- (B) one or two charged leptons (“Leptonic Channel”), or
- (C) a $\nu\bar{\nu}$ pair (“Missing Energy Channel”).

Photons were identified as clusters in the electromagnetic calorimeter (EC) which were not associated with tracks if the lateral spread of the clusters satisfied the criteria described in reference [10]. The efficiencies were increased by approximately 10 – 20% by including photon conversions into e^+e^- pairs using the methods described in reference [9].

The dominant background to the searches arises from ISR producing mostly low-energy photons along the beam direction. Therefore, we required the two highest-energy photons in the event to satisfy the following:

- (G1) The two photon candidates were required to be in the fiducial region $|\cos(\theta_\gamma)| < 0.875$, where the polar angle θ_γ is the angle of the photon with respect to the e^- beam direction.
- (G2) The highest-energy photon was required to have $E_{\gamma 1}/E_{\text{beam}} > 0.10$ and the second-highest-energy photon was required to have $E_{\gamma 2}/E_{\text{beam}} > 0.05$.
- (G3) The sum of track momenta and extra electromagnetic cluster energies in a 15 degree cone about the photons had to be less than 2 GeV.

The remaining cuts depend on the particular recoil topologies. In order to assess the background modelling, the photon cuts are not applied until after preselection cuts for the three final state topologies. For all topologies, tracks and EC clusters that are not associated to tracks are required to satisfy the criteria defined in reference [30]. The criteria for the definition of tracks and EC clusters in the OPAL detector are described in reference [31].

3.1 Hadronic Channel

The hadronic channel is characterised by two photons recoiling against a hadronic system. Candidate events were required to satisfy the following criteria:

- (A1) The standard OPAL hadronic event preselection in Ref. [32]; $R_{\text{vis}} > 0.5$; $|\Sigma p_z^{\text{vis}}| < 0.6E_{\text{beam}}$; and at least two electromagnetic clusters with $E/E_{\text{beam}} > 0.05$. The quantities E_{vis} and \vec{p}_{vis} are the scalar and vector sums of track momenta, unassociated EC and unassociated hadron calorimeter cluster energies, and $R_{\text{vis}} \equiv \frac{E_{\text{vis}}}{E_{\text{cm}}}$. The visible momentum along the beam direction, obtained from the sum of all tracks and unassociated clusters, is denoted by $|\Sigma p_z^{\text{vis}}|$.
- (A2) The photon pair criteria G1–G3.
- (A3) Photon isolation: both photon candidates were required to satisfy $p_{\text{T, jet-}\gamma} > 5$ GeV, where $p_{\text{T, jet-}\gamma}$ is the photon momentum transverse to the axis of the closest jet out of two jets formed with the Durham [33] scheme (excluding the photon pair).
- (A4) Photon energy balance: $(E_{\gamma 1} - E_{\gamma 2})/E_o < 0.5$, where $E_o \equiv (s - M_Z^2)/(2\sqrt{s})$ would be the energy of a single photon recoiling from the Z^0 . This cut discriminates against ISR photon pairs.
- (A5) The recoil mass from the di-photon system, M_{recoil} , is required to be consistent with the Z^0 : $|M_{\text{recoil}} - M_Z| < 20$ GeV (not used in the *general* search mode).

3.2 Charged Lepton Channel

This channel searches for events in the $\gamma\gamma\ell^+\ell^-$ final state. Events having only one well-identified lepton are accepted to avoid efficiency loss for lepton tracks at low polar angles. The lepton tracks are treated as jets to include tau lepton final state topologies. Leptonic channel candidates were required to satisfy the following criteria:

- (B1) The standard OPAL low multiplicity preselection of Ref. [34]; $R_{\text{vis}} > 0.2$; $|\Sigma p_z^{\text{vis}}| < 0.8E_{\text{beam}}$; number of EC clusters not associated with tracks ≤ 10 ; number of tracks N_{T} satisfies $1 \leq N_{\text{T}} \leq 7$; at least two electromagnetic clusters with $E/E_{\text{beam}} > 0.05$.
- (B2) The photon pair criteria G1–G3.
- (B3) For events having only one track and a converted photon, the EC cluster associated with the track must not also be associated with the conversion.
- (B4) For events having two or more tracks, the event is forced to have two jets within the Durham scheme, excluding the identified di-photon candidate, and both jets are required to have energies above 3 GeV.
- (B5) $|M_{\text{recoil}} - M_Z| < 20$ GeV (not used in the *general* search mode).

3.3 Missing Energy Channel

The missing energy channel is characterised by two photons and no other significant detector activity. Candidates in the missing energy channel were required to satisfy the following criteria:

- (C1) The standard OPAL low multiplicity preselection of Ref. [34]; the vetoes in Ref. [35] against cosmic ray and beam-wall/beam-gas backgrounds; number of EC clusters not associated with tracks ≤ 4 ; number of tracks ≤ 3 ; $|\Sigma p_z^{\text{vis}}| < 0.8E_{\text{beam}}$; and at least two electromagnetic clusters with $E/E_{\text{beam}} > 0.05$.

- (C2) The photon pair criteria G1–G3.
- (C3) $p_T(\gamma\gamma) > 0.05E_{\text{beam}}$ where $p_T(\gamma\gamma)$ is the transverse momentum of the di-photon system; the angle between the two photons in the plane transverse to the beam axis: $|\phi_{\gamma\gamma} - 180^\circ| > 2.5^\circ$; the polar angle of the momentum of the di-photon system: $|\cos\theta_{\gamma\gamma}| < 0.966$.
- (C4) No track candidates other than those associated with an identified photon conversion.
- (C5) Veto on unassociated calorimeter energy: the energy observed in the EC not associated with the two photons is required to be less than 3 GeV.
- (C6) $|M_{\text{recoil}} - M_Z| < 20$ GeV (not used in the *general* search mode).

4 Results

For the 1999 and 2000 data, the numbers of events passing the cuts are listed for the three recoil topologies in Table 2. There are no events in which more than one photon pair satisfying the cuts was found. The numbers of candidates passing cuts are generally in good agreement with the expected numbers of Standard Model backgrounds; this was also the case in earlier OPAL publications for the lower E_{cm} [8–11]. The one noteworthy discrepancy is for cut C1 in the missing energy channel. In this channel there is a large background from Bhabha electrons lost in the beampipe. The ISR photons for this background have a steeply rising population in the forward direction. Cut C1 is made before the cut on polar angle, and therefore a discrepancy arises because of the steep angular distribution and the inadequate modelling of material in the very low polar angle regions.

Combining both the 1999 and 2000 data in the three topologies, 112 candidates pass the *general* cuts compared to 118.3 ± 7.9 expected background, and 42 candidates pass the h^0Z^0 cuts compared to 51.9 ± 2.9 expected background.

4.1 Systematic Errors

The uncertainty on the modelling of ISR is the most important component of the systematic error because of the irreducible background arising from this process. This uncertainty is estimated from the comparison of data with the Standard Model background simulation for events passing cuts A2, B2, or C2. The shapes of the distributions for $E_{\gamma 1}$ and $E_{\gamma 2}$ are modelled well by the simulations. The simulations also reproduce well the number of events observed in the three channels combined. For the 1999 and 2000 runs the simulations predict 3.7% and 5.0% fewer events than observed, respectively. The statistical error on the 1999 data is 4%, and similarly for the 2000 data. Modelling of photon conversions has an uncertainty of approximately 1%. Uncertainties on the integrated luminosities of the data sets are negligible compared to the other uncertainties. Combined, these error sources result in a total background uncertainty estimate of 10%. The experimental results which follow are not very sensitive to this number.

The dominant systematic uncertainty for the signal acceptances arises from the photon detection efficiency, primarily due to the simulation of the photon isolation criterion G3 [11], and is estimated to be 3%. The uncertainty from Monte Carlo statistics is typically better than 4%. A systematic error on the photon energy scale is estimated by comparing the fitted single-photon ISR energy peak to the expected value based on the precisely known beam energy and Z^0 mass. For this study a sample of single-photon events was generated and compared to the data for photon energies above 5 GeV and polar angles greater than 25 degrees. This leads to a systematic uncertainty on the di-photon mass of 0.35 GeV at a mass of 100 GeV. The resolution on the di-photon mass ranges from approximately 0.5 GeV at $m_{\gamma\gamma} = 10$ GeV to 2.3 GeV at $m_{\gamma\gamma} = 100$ GeV.

4.2 General Search Results

Figure 1 shows the di-photon mass versus the recoil mass for all candidate events passing the *general* search cuts for the year 2000 data only (where all the data were taken at E_{cm} near 206 GeV). The events at recoil masses near zero are expected from $e^+e^- \rightarrow \gamma\gamma$ background. This plot also shows no unexpected structure for the lower E_{cm} data. In the absence of an indication for signal, limits are placed on the production at $E_{\text{cm}} \sim 206$ GeV of a massive state decaying into photon pairs.

For the *general* search, the system recoiling from the di-photon system is not assumed to be a Z^0 and hence the branching fractions $X \rightarrow \gamma\gamma$ and Y into topology A, B or C are not uniquely predicted. Here X is a scalar particle and Y is a scalar or vector particle. Furthermore, X and Y must be short-lived particles so that they decay near the interaction point. In order to be independent of models we do not combine data from different E_{cm} and therefore we restrict this part of the analysis to the highest energy data, in the E_{cm} range of 205–207 GeV; this represents 200.0 pb^{-1} of the 2000 data. We choose to present upper limits on $\sigma(e^+e^- \rightarrow XY) \times B(X \rightarrow \gamma\gamma) \times B(Y \rightarrow \text{ff})$ as a function of M_X . When presenting production upper limits as functions of M_X , we show the limit obtained for the value of M_Y that gives the smallest efficiency in the region $M_Z - M_X < M_Y < E_{\text{cm}} - M_X$. The lower bounds on M_Y are used because searches for di-photon resonances at LEP1 [11, 36, 37] have already set good limits on the lower-mass phase space. M_X and M_Y are also required to be above 10 GeV and below 200 GeV in order to allow the decay products to have sufficient energies and momenta to give reasonable search acceptances at $E_{\text{cm}} = 206$ GeV. For a scalar/vector hypothesis for X/Y , the efficiency is found to be the same to within 5% as that for a scalar/scalar hypothesis; the lower of these efficiencies is used in setting the limits. For the lepton search channel, the efficiency for $Y \rightarrow \tau^+\tau^-$ is used, as it turns out to have the lowest of the dilepton efficiencies.

The event candidates from $E_{\text{cm}} = 205 - 207$ GeV in the *general* search are used to calculate 95% CL upper limits on the number of events in 1 GeV $[M_X, M_Y]$ mass bins. The acceptances used at each 1 GeV mass bin are obtained by interpolation using a 4th-order polynomial fit to the acceptances simulated on a 5 GeV grid. For each $[M_X, M_Y]$ bin, the 95% CL upper limit on the number of signal events is computed using the frequentist method of reference [38], which takes into account the predicted Standard Model background. This statistical procedure also incorporates the di-photon mass resolution (typically less than 2 GeV for $m_{\gamma\gamma} < 100$ GeV); the limit procedure is valid for resonance states narrower than this resolution. The effect of the 10% systematic error for background modelling is incorporated in the statistical procedure, as is the 4% uncertainty on signal. For these *general* search limits, an additional systematic uncertainty of 5% is added to the signal uncertainty to account for interpolation error in the efficiency grid (especially near kinematic limits) and for the differences in the acceptance calculations for the scalar versus vector nature of particle Y .

Figure 2 shows the 95% CL upper limits on $\sigma(e^+e^- \rightarrow XY) \times B(X \rightarrow \gamma\gamma) \times B(Y \rightarrow \text{ff})$. These results are valid independent of the nature of Y , provided it decays to two jets, a lepton pair, or missing energy, and has a width less than or equal to the experimental resolution. Limits of 25 – 60 fb are obtained over $10 < M_X < 180$ GeV. The limits for the leptonic final state are stronger, except in the case Y couples exclusively to $\tau^+\tau^-$ (the final state with lowest acceptance).

4.3 Limits on h^0Z^0 with $h^0 \rightarrow \gamma\gamma$

The distribution of di-photon masses for the h^0Z^0 search candidates for the 1999 data ($E_{\text{cm}} = 192 - 202$ GeV) and the 2000 data ($E_{\text{cm}} = 200 - 209$ GeV) is shown in Figure 3a together with

the simulation of Standard Model backgrounds. The observation of 42 events is in reasonable agreement with the expected background of 51.9 ± 2.9 events. Because the $h^0 Z^0$ process has a production rate and branching fractions described by theory, the data taken at all LEP energies can be combined in this analysis. Figure 3b shows the distribution of $m_{\gamma\gamma}$ for $E_{\text{cm}} = 88 - 209$ GeV. This plot is restricted to $m_{\gamma\gamma}$ larger than 20 GeV because there is no background estimate for the low- $m_{\gamma\gamma}$ LEP1 data. The figure has no indication of a resonance, and the total of 124 candidates agrees with the predicted background of 135.2 ± 10.8 events.

Also indicated on Figure 3 is the hypothetical signal of a 100 GeV Higgs boson produced at Standard Model strength and decaying into di-photons with a branching fraction of 18% – the fraction predicted in the “benchmark fermiophobic model” calculated by simply turning off the Higgs-fermion coupling. In reality, the fermiophobic Higgs photon branching ratio depends on parameters and details of fermiophobic 2HDM models [4,5], so this benchmark is simply a guide to the broad interpretation of the data. Here we use the HDECAY [39] package to calculate the modified photonic branching fractions.

The events passing all $h^0 Z^0$ cuts are used to set an upper limit on the di-photon branching ratio for a particle produced in association with a Z^0 and having the Standard Model Higgs boson production rate. As described in the previous section, the frequentist method of reference [38] is used to determine the 95% confidence level upper limit on possible signal events at each di-photon mass. Figure 4 shows the 95% CL upper limit for the di-photon branching ratio obtained by combining the candidate events in 1999 and 2000 data described in this paper with those from OPAL searches at $\sqrt{s} = 88 - 189$ GeV [8,9,11], where the Standard Model $h^0 Z^0$ production cross-section is assumed at each centre-of-mass energy. Higgs bosons produced at Standard Model rate and decaying exclusively to di-photons are ruled out at the 95% confidence level over the mass range 20 – 117 GeV. Figure 4 also shows the $h^0 \rightarrow \gamma\gamma$ branching ratio computed using HDECAY with the fermionic couplings switched off; the photonic branching fraction falls as the W^+W^- and $Z^0 Z^0$ channels become kinematically favourable. A 95% CL lower mass limit for the benchmark fermiophobic Higgs bosons is set at 105.5 GeV, where the predicted branching ratio crosses the upper-limit curve. The median limit one would expect to obtain in an ensemble of experiments in the absence of a signal is 106.4 GeV. The benchmark fermiophobic branching ratios can also be calculated using the HZHA3 [29] generator. HZHA3 produces slightly higher di-photon branching fractions than does HDECAY. The lower mass limit on the benchmark fermiophobic Higgs boson calculated with HZHA3 is 106.3 GeV.

5 Conclusions

A search for the production of Higgs bosons and other new particles of width no larger than the experimental resolution and decaying to photon pairs has been performed using e^+e^- annihilation data with $E_{\text{cm}} = 192 - 209$ GeV combined with 88 – 189 GeV data from previous OPAL searches. Model independent upper limits are obtained for $E_{\text{cm}} \sim 206$ GeV on $\sigma(e^+e^- \rightarrow XY) \times B(X \rightarrow \gamma\gamma) \times B(Y \rightarrow f\bar{f})$, where limits of 25–60 fb are obtained over $10 < M_X < 180$ GeV, for $10 < M_Y < 200$ GeV and $M_X + M_Y > M_Z$. The limits are valid for Y either a scalar or vector particle, provided that the Y decays to a fermion pair (interpreted as two jets, a lepton pair, or missing energy).

Using OPAL data from all LEP centre-of-mass energies, model-specific limits are placed on $B(h^0 \rightarrow \gamma\gamma)$ up to a Higgs boson mass of 117 GeV, provided the Higgs particle is produced via $e^+e^- \rightarrow h^0 Z^0$ at the Standard Model rate. A lower mass bound of 105.5 GeV is set at the 95% confidence level for benchmark fermiophobic Higgs bosons. Similar lower mass limits on benchmark fermiophobic Higgs bosons have been obtained by the other LEP experiments [12–14].

Acknowledgements:

We thank A. G. Akeroyd, L. Brücher, and R. Santos for helpful discussions. We particularly wish to thank the SL Division for the efficient operation of the LEP accelerator at all energies and for their close cooperation with our experimental group. In addition to the support staff at our own institutions we are pleased to acknowledge the
Department of Energy, USA,
National Science Foundation, USA,
Particle Physics and Astronomy Research Council, UK,
Natural Sciences and Engineering Research Council, Canada,
Israel Science Foundation, administered by the Israel Academy of Science and Humanities,
Benozio Center for High Energy Physics,
Japanese Ministry of Education, Culture, Sports, Science and Technology (MEXT) and a grant under the MEXT International Science Research Program,
Japanese Society for the Promotion of Science (JSPS),
German Israeli Bi-national Science Foundation (GIF),
Bundesministerium für Bildung und Forschung, Germany,
National Research Council of Canada,
Hungarian Foundation for Scientific Research, OTKA T-029328, and T-038240,
Fund for Scientific Research, Flanders, F.W.O.-Vlaanderen, Belgium.

References

- [1] J. Ellis, M.K. Gaillard, and D.V. Nanopoulos, Nucl. Phys. **B106** (1976) 292.
- [2] K. Hagiwara and M.L. Stong, Z. Phys. **C62** (1994) 99.
- [3] A. Stange, W. Marciano and S. Willenbrock, Phys. Rev. **D49** (1994) 1354.
- [4] A.G. Akeroyd, Phys. Lett. **B368** (1996) 89.
- [5] L. Brücher, R. Santos, Eur. Phys. J. **C12** (2000) 87.
- [6] J.F. Gunion, R. Vega and J. Wudka, Phys. Rev. **D42** (1990) 1673.
- [7] H. Haber, G. Kane and T. Sterling, Nucl. Phys. **B161** (1979) 493.
- [8] OPAL Collab., G. Abbiendi *et al.*, Phys. Lett. **B464** (1999) 311.
- [9] OPAL Collab., K. Ackerstaff *et al.*, Phys. Lett. **B437** (1998) 218.
- [10] OPAL Collab., K. Ackerstaff *et al.*, Eur. Phys. J. **C1** (1998) 31.
- [11] OPAL Collab., P. Acton *et al.*, Phys. Lett. **311** (1993) 391.
- [12] ALEPH Collab., CERN-EP-2002-044, submitted to Phys. Lett. B.
- [13] DELPHI Collab., P. Abreu *et al.*, Phys. Lett. **B507** (2001) 89.
- [14] L3 Collab., P. Achard *et al.*, Phys. Lett. **B534** (2002) 28.
- [15] D0 Collab., B. Abbott *et al.*, Phys. Rev. Lett. **82** (1999) 2244.
- [16] CDF Collab., T. Affolder *et al.*, Phys. Rev. **D64** (2001) 092002.

- [17] OPAL Collab., K. Ahmet *et al.*, Nucl. Instr. Meth. **A305** (1991) 275;
O. Biebel *et al.*, Nucl. Instr. Meth. **A323** (1992) 169;
M. Hauschild *et al.*, Nucl. Instr. Meth. **A314** (1992) 74;
S. Anderson *et al.*, Nucl. Instr. Meth. **A403** (1998) 326.
- [18] J. Allison *et al.*, Nucl. Instr. Meth. **A305** (1992) 47.
- [19] S. Jadach, B.F. Ward and Z. Was, Phys. Rev. **D63** (2001) 113009.
- [20] T. Sjöstrand *et al.*, Comp. Phys. Comm. **135** (2001) 238.
- [21] J. Fujimoto *et al.*, Comp. Phys. Comm. **100** (1997) 128.
- [22] M. Skrzypek *et al.*, Comp. Phys. Comm. **94** (1996) 216;
M. Skrzypek *et al.*, Phys. Lett. **B372** (1996) 289.
- [23] S. Jadach, W. Placzek and B. F. L. Ward, Phys. Lett. **B390** (1997) 298.
- [24] D. Karlen, Nucl. Phys. **B289** (1987) 23.
- [25] S. Jadach *et al.*, Comp. Phys. Comm. **66** (1991) 276.
- [26] G. Montagna *et al.*, Nucl. Phys. **B541** (1999) 31.
- [27] F.A. Berends and R. Kleiss, Nucl. Phys. **B186** (1981) 22.
- [28] S. Jadach, Z. Was, Comp. Phys. Comm. **76** (1993) 361.
- [29] P. Janot, in *Physics at LEP2*, edited by G. Altarelli, T. Sjöstrand and F. Zwirner, CERN 96-01 Vol. 2 p.309.
For version 3, see <http://alephwww.cern.ch/~janot/Generators.html>.
- [30] OPAL Collab., G. Alexander *et al.*, Z. Phys. **C72** (1996) 191.
- [31] OPAL Collab., G. Abbiendi *et al.*, Eur. Phys. J. **C19** (2001) 587.
- [32] OPAL Collab., G. Alexander *et al.*, Z. Phys. **C52** (1991) 175.
- [33] N. Brown and W.J. Stirling, Phys. Lett. **B252** (1990) 657;
S. Bethke, Z. Kunszt, D. Soper and W.J. Stirling, Nucl. Phys. **B370** (1992) 310;
S. Catani *et al.*, Phys. Lett. **B269** (1991) 432;
N. Brown and W.J. Stirling, Z. Phys. **C53** (1992) 629.
- [34] OPAL Collab., R. Akers *et al.*, Z. Phys. **C61** (1994) 19.
- [35] OPAL Collab., R. Akers *et al.*, Z. Phys. **C65** (1995) 47.
- [36] DELPHI Collab., P. Abreu *et al.*, Phys. Lett. **B458** (1999) 431;
DELPHI Collab., P. Abreu *et al.*, Z. Phys. **C72** (1996) 179.
- [37] L3 Collab., M. Acciarri *et al.*, Phys. Lett. **388** (1996) 409;
L3 Collab., O. Adriani *et al.*, Phys. Lett. **295** (1992) 337.
- [38] T. Junk, Nucl. Instr. Meth. **A434** (1999) 435.
- [39] A. Djouadi, J. Kalinowski and M. Spira, Comp. Phys. Comm. **108** (1998) 56.

Run (year)	Integrated Luminosity (pb^{-1})	E_{cm} (GeV)
1990-95	173.00	88 – 94
1995	5.41	130 – 140
1996	10.32	172.3
1996	10.04	161.3
1997	57.73	182.6
1998	182.61	188.6
1999	28.90	191.6
1999	74.79	195.6
1999	77.21	199.6
1999	36.08	201.6
2000	0.82	200 – 202
2000	2.62	202 – 204
2000	76.81	204 – 206
2000	123.26	206 – 208
2000	7.54	208 – 210

Table 1: Summary of all data sets used in the searches. Results using data from 1990 – 1998 were reported in earlier publications [8–11].

Cut	Data	ΣBkgd	$(\gamma/Z)^*$	4f				ϵ_{100} (%)
1999 Hadronic Channel								
(A1)	10645	10695.4	7535.0	3160.2				70
(A2)	62	56.1	53.6	2.6				62
(A3)	48	44.8	42.5	2.3				61
(A4)	29	22.0 ± 1.8	19.8	2.2				61
(A5)	15	10.9 ± 0.9	10.9	0.0				60
2000 Hadronic Channel								
(A1)	9371	9152.4	6096.0	3056.2				71
(A2)	52	46.5	43.5	3.0				60
(A3)	39	38.3	36.0	2.3				60
(A4)	18	17.8 ± 1.6	15.7	2.1				58
(A5)	7	7.9 ± 0.7	7.8	0.1				57
Cut	Data	ΣBkgd	e^+e^-	$\tau^+\tau^-$	$\mu^+\mu^-$	$\gamma\gamma$	e^+e^-ff	ϵ_{100} (%)
1999 Leptonic Channel								
(B1)	41947	39060.6	37245.9	715.6	50.5	314.6	734.0	82
(B2)	167	188.6	72.4	11.3	8.0	95.5	1.5	69
(B3)	155	178.8	67.3	10.4	7.4	92.4	1.2	63
(B4)	23	31.4 ± 5.8	18.8	5.0	6.9	0.4	0.3	50
(B5)	5	9.2 ± 1.7	4.6	1.7	2.9	0.0	0.0	48
2000 Leptonic Channel								
(B1)	37432	33928.9	32329.1	607.8	43.7	273.9	674.4	82
(B2)	138	146.6	57.6	10.2	6.8	70.9	1.0	71
(B3)	123	141.7	55.4	9.2	6.4	69.7	1.0	67
(B4)	28	23.7 ± 4.8	13.0	4.4	5.9	0.2	0.3	61
(B5)	11	9.8 ± 2.0	5.1	1.9	2.6	0.0	0.0	52
Cut	Data	ΣBkgd	$\nu\bar{\nu}\gamma\gamma$	$\gamma\gamma$	e^+e^-	$\ell^+\ell^-$	e^+e^-ff	ϵ_{100} (%)
1999 Missing Energy Channel								
(C1)	224989	129713.4	50.5	3337.7	124769.9	157.4	1397.9	88
(C2)	377	336.3	13.0	276.4	45.1	1.1	0.7	75
(C3)	71	73.1	12.2	31.5	27.8	1.0	0.5	69
(C4)	33	42.4	12.1	29.2	0.9	0.0	0.2	69
(C5)	8	12.9 ± 0.5	11.4	0.3	0.9	0.0	0.2	67
(C6)	3	7.6 ± 0.3	7.5	0.0	0.0	0.0	0.1	66
2000 Missing Energy Channel								
(C1)	202649	113268.8	43.9	2737.6	109070.9	136.8	1279.7	87
(C2)	345	315.1	11.5	267.5	34.6	0.9	0.5	75
(C3)	66	62.1	11.0	30.1	19.7	0.8	0.3	70
(C4)	34	39.0	11.0	27.8	0.0	0.0	0.2	69
(C5)	6	10.5 ± 0.5	10.2	0.1	0.0	0.0	0.1	68
(C6)	1	6.5 ± 0.3	6.5	0.0	0.0	0.0	0.0	65

Table 2: The $h^0 \rightarrow \gamma\gamma$ searches: events from the 1999 and 2000 data remaining after the indicated cumulative cuts. Hadronic channel cuts (A), leptonic channel cuts (B), and missing energy channel cuts (C) are described in Sections 3.1, 3.2, and 3.3, respectively. The entries for A5, B5, C6 are for the M_{recoil} cut for the h^0Z^0 search; they are not applied in the *general* search. The uncertainty shown indicates statistical error only; the systematic uncertainty is approximately 10%. In (A), the components from $(\gamma/Z)^*$ and four-fermion (“4f”) final states are shown. In (B), the components from Bhabha scattering (e^+e^-), τ -pair, μ -pair, $\gamma\gamma$ and e^+e^-ff final states are shown. In (C), the components from $\nu\bar{\nu}\gamma\gamma$, $\gamma\gamma$, e^+e^- -pair, lepton pair ($\ell \equiv \mu, \tau$) production and e^+e^-ff final states are shown. The efficiencies for detection of a 100 GeV Higgs boson are shown in the last column.

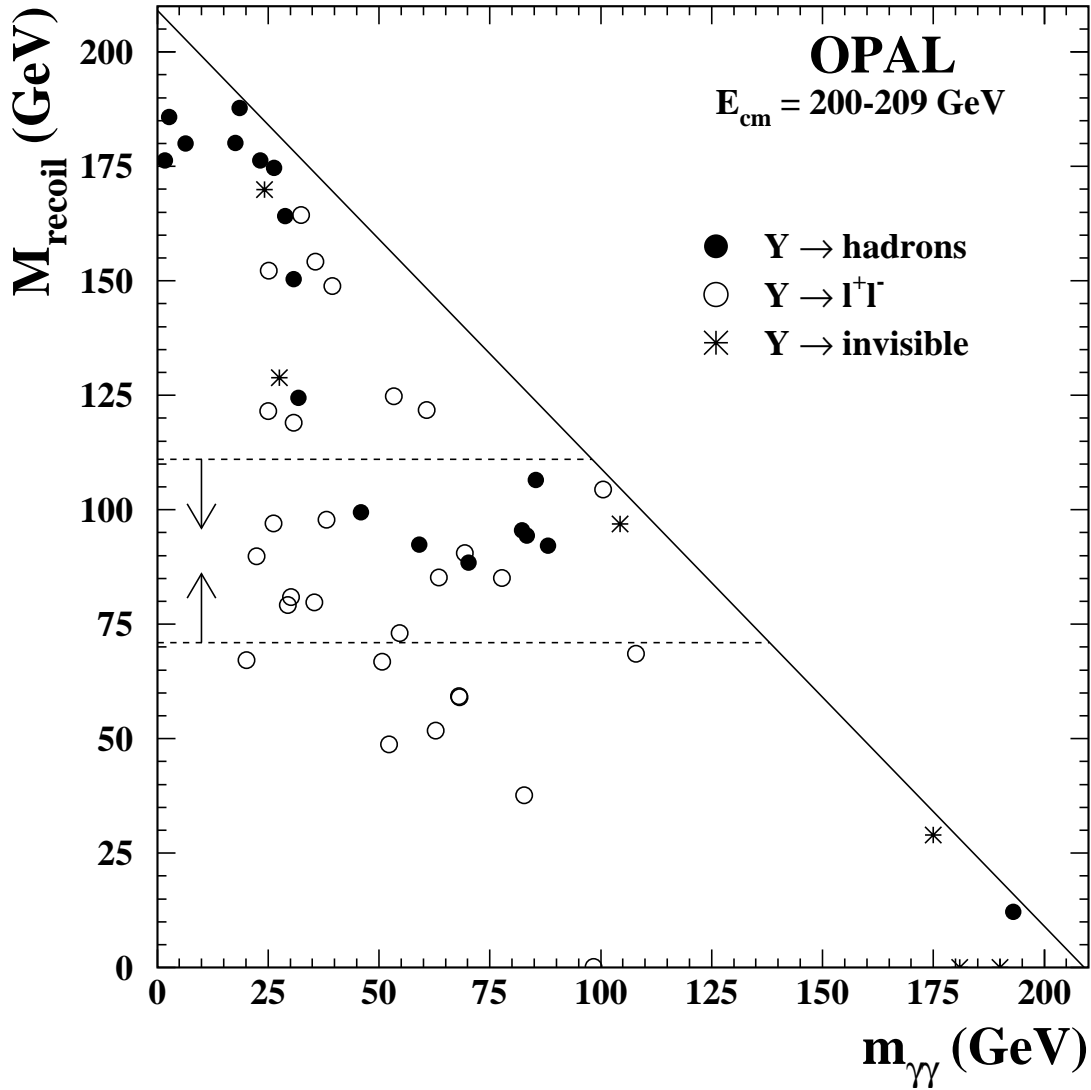


Figure 1: Distribution of mass recoiling against the di-photon system, M_{recoil} , versus di-photon invariant mass, $m_{\gamma\gamma}$, for events passing the *general* search cuts on the Y2000 data. The different search channels are as indicated. The diagonal line denotes the kinematic limit. Dashed lines and arrows indicate the events accepted for the h^0Z^0 search.

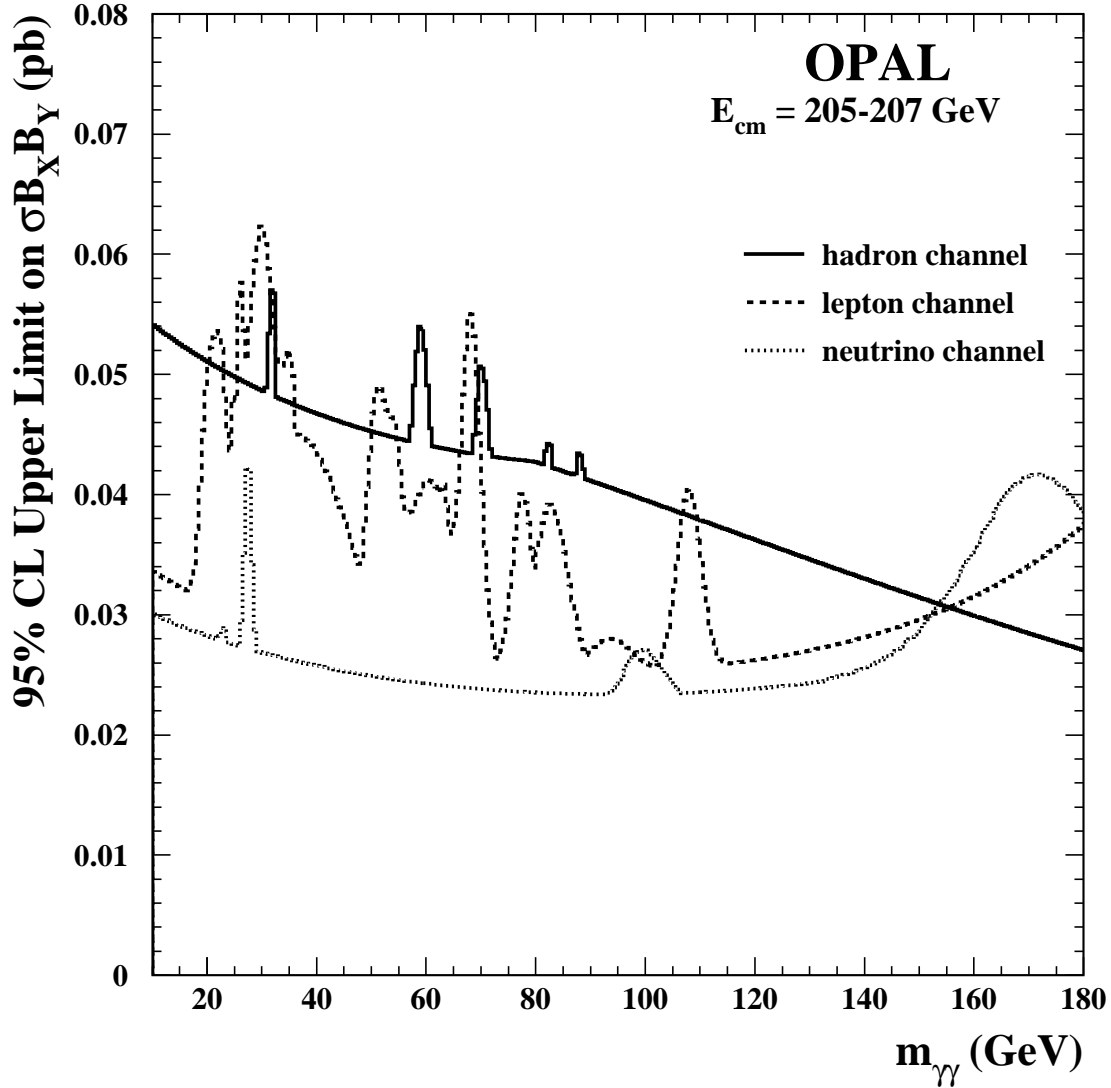


Figure 2: For data taken at $E_{\text{cm}} \sim 206$ GeV: 95% confidence level upper limit on $\sigma(e^+e^- \rightarrow XY) \times B(X \rightarrow \gamma\gamma) \times B(Y \rightarrow f\bar{f})$ for the cases where Y decays hadronically (solid line), Y decays into a charged lepton pair (dashed line), and Y decays invisibly (dotted line). The limits for each M_X assume the smallest efficiency as a function of M_Y such that $10 < M_Y < 200$ GeV and that $M_X + M_Y > M_Z$.

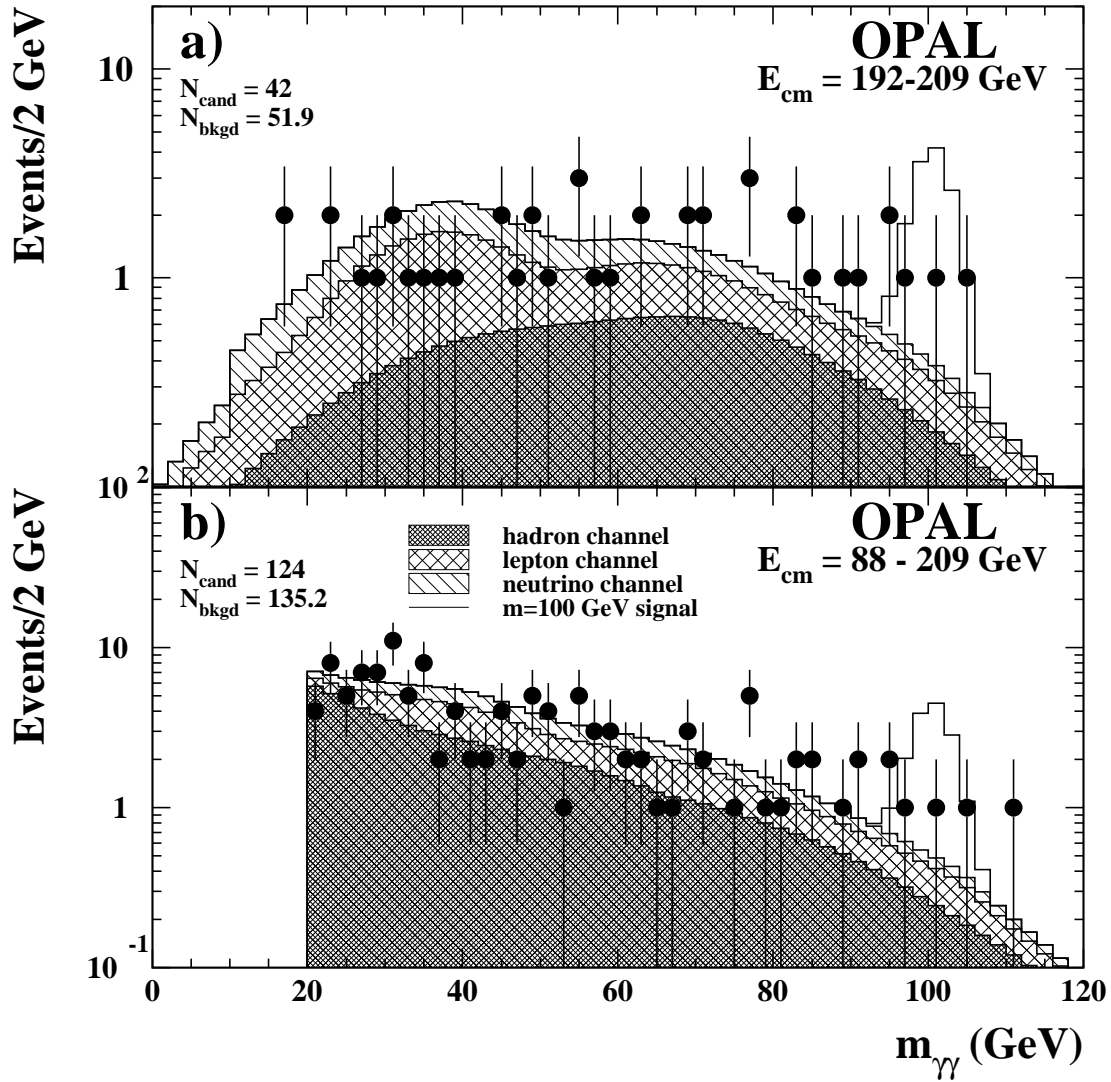


Figure 3: Distribution of mass of the two highest-energy photons in the $h^0 Z^0$ search after application of all selection criteria. a) shows the data taken in 1999 and 2000 only, while b) shows the data taken at all energies. Data are shown as points with error bars. Background simulation is shown as a histogram showing the contributions from the hadronic, charged lepton and missing energy channels as denoted. The expected signal for a 100 GeV fermiophobic Higgs boson produced with Standard Model strength is also shown.

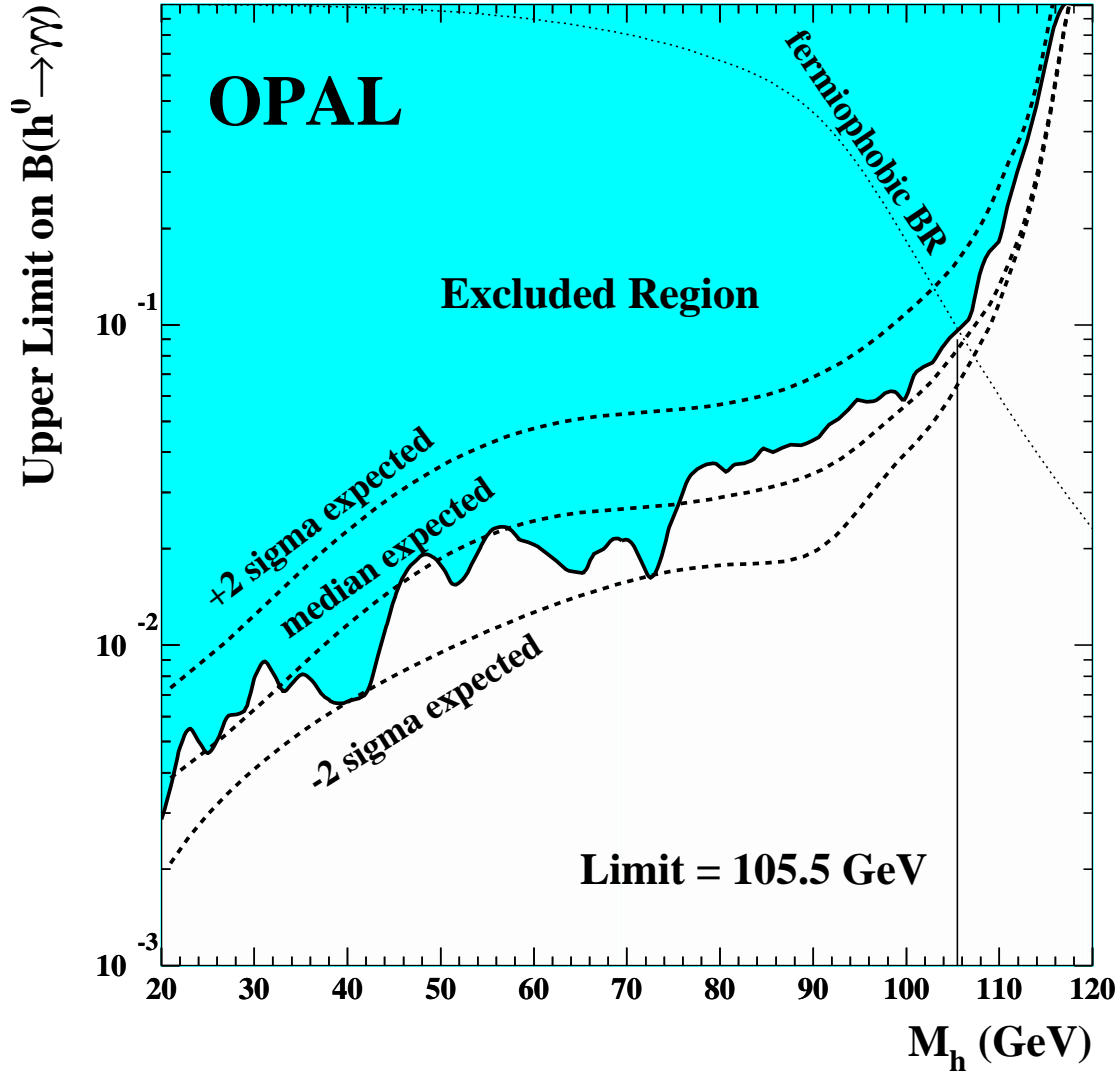


Figure 4: 95% confidence level upper limit on the branching fraction $B(h^0 \rightarrow \gamma\gamma)$ for a Standard Model Higgs boson production rate. The shaded region, obtained with all LEP energies, is excluded. The dotted line is the predicted $B(h^0 \rightarrow \gamma\gamma)$ assuming $B(h^0 \rightarrow f\bar{f}) = 0$. The intersection of the dotted line with the exclusion curve gives a lower limit of 105.5 GeV for the fermiophobic Higgs model. The median expected limit and the $\pm 2\sigma$ range of expected limits are indicated by the dashed lines.